This is an open access article published under an ACS AuthorChoice License, which permits copying and redistribution of the article or any adaptations for non-commercial purposes.

ACS OMEGA

Article

Cite This: ACS Omega 2018, 3, 4412−4417

Surface State Passivation and Optical Properties Investigation of GaSb via Nitrogen Plasma Treatment

Xuan Fang,[†] Zhipeng Wei,*[,†] Dan Fang,[†] Xueying Chu,[†] Jilong Tang,[†] Dengkui Wang,[†] Xinwei Wang,[†] Jinhua Li,[†] Yongfeng Li,[§] Bin Yao,[§] Xiaohua Wang,[†] and Rui Chen*[,‡]

[†]State Key Laboratory of High Power Semiconductor Lasers, School of Science, Changchun University of Science and Technology, 7089 Wei-Xing Road, Changchun 130022, P. R. China

[‡]Department of Electrical and Electronic Engineering, South University of Science and Technology of China, Shenzhen, Guangdong 518055, P. R. China

[§]Key Laboratory of Physics and Technology for Advanced Batteries, Ministry of Education, College of Physics, Jilin University, Changchun 130012, P. R. China

Supporting Information

ABSTRACT: GaSb is one of the most suitable semiconductors for optoelectronic devices operating in the mid-infrared range. However, the existence of GaSb surface states has dramatically limited the performance of these devices. Herein, a controllable nitrogen passivation approach is proposed for GaSb. The surface states and optical properties of GaSb were found to depend on the N passivation conditions. Varying the plasma power during passivation modified the chemical bonds of the GaSb surface, which influenced the emission efficiency. X-ray photoelectron spectroscopy was used to quantitatively demonstrate that the GaSb oxide layer was removed via treatment at a plasma power of 100 W. After nitrogen passivation, the samples exhibited enhanced emission. Free exciton emission was the main factor leading to this enhanced luminescence. An energy band model for the surface states is used to explain the carrier radiative recombination processes. This nitrogen passivation approach can suppress surface states and improve the surface quality of GaSb-based materials and devices. The enhancement in exciton-related emission by this simple approach is important for improving the performance of GaSb-based optoelectronic devices.

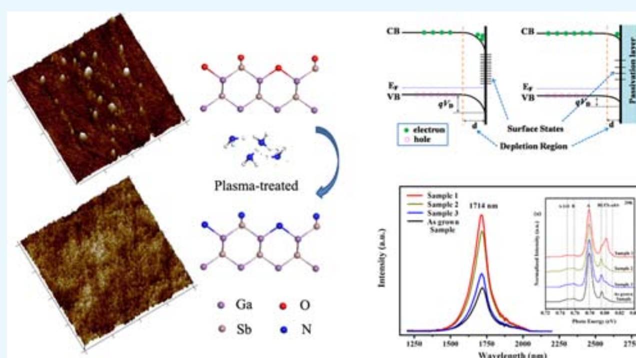

1. INTRODUCTION

The superficial and interfacial characteristics are important for the performance of advanced semiconductor devices, which are gaining increasing interest in optoelectronics.[1−5] Surface states are generally induced by the rebonding of surface dangling bonds (such as forming surface oxides) and surface contamination (such as the adsorption of gas molecules).[6,7] The presence of these surface states leads to poor photoelectric efficiency of these devices, so the passivation of surface states has become an important research focus for practical applications. Investigations of surface passivation have been intensively carried out for traditional semiconductors such as II−VI and III−V materials and for more modern materials such as two-dimensional and perovskite materials.[3,8−14] These studies have shown that the properties of semiconductors and the performances of devices can be improved by optimizing the surface passivation.

III−V materials possess highly reactive surfaces and a high amount of dangling bonds, so they exhibit a high density of surface states.[15−18] This is especially true for GaSb. The performance of GaSb-based devices is suppressed by the presence of surface states,[19,20] which limit the application of GaSb-based devices. Much effort has been focused on reducing the surface states of GaSb. These have included incorporating interfacial or capping layers composed of wide band gap materials, wet chemistry modification approaches, in situ hydrogen plasma treatment, and the deposition of high-*k* dielectrics.[19,21−23] Sulfur (S) passivation has long been recognized as a useful method for removing surface states.[24,25]

By adjusting the treatment conditions, the oxide layer and surface dangling bonds can be effectively etched or filled.[26−28] Unfortunately, these solution-based processing techniques still leave some residual oxides and can further degrade the structural quality of the materials. To overcome this, H_2S predeposition annealing has been proposed, which can provide solid S passivation with strong resistance to oxidation, compared with $(NH_4)_2S$ solution treatment.[29−31]

Received: November 13, 2017
Accepted: March 19, 2018
Published: April 24, 2018

© 2018 American Chemical Society

DOI: 10.1021/acsomega.7b01783
ACS Omega 2018, 3, 4412−4417

Like S, nitrogen (N) should also be a suitable candidate for passivation. N is more electronegative (3.08) than S (2.58), so it should be able to more effectively fill surface dangling bonds. Guo et al.[32] proposed N substitution at the high-*k*/GaAs interface for minimizing interfacial diffusion and defect states. Alekseev et al. demonstrated that $N_2H_4{\cdot}H_2O$ wet chemistry passivation could reduce the surface state density of GaAs nanowires.[33] N passivation is also effective for overcoming problems associated with surface states in InP-based materials.

In the present study, the N passivation of GaSb based on plasma-enhanced atomic layer deposition (PEALD) is proposed and realized. Controllable N passivation consisting of atomic layer etching and N bonding processes is achieved during PEALD, using NH_3 as an N source. X-ray photoelectron spectroscopy (XPS) is used to demonstrate that the removal of surface states depends on the power of the N plasma. The influence of N passivation on the luminescence mechanism is discussed, based on the results of photoluminescence (PL) measurements.

2. RESULTS AND DISCUSSION

Figure 1 shows room-temperature PL spectra of the GaSb samples with and without N passivation. The emission at approximately 1714 nm was assigned to the near band gap emission (NBE) of GaSb.[34] After N passivation, the emission intensity of the samples changed significantly. For example, the emission intensity of sample 1 was approximately three times higher than that of the as-grown GaSb. The factor of emission enhancement was sensitive to the power of the N plasma, as shown in the inset in Figure 1. Figure S1 shows normalized PL spectra. The full-width at half-maximum values of the emissions of the four samples were all 50 meV. This implied that the samples possessed the same emission mechanism.[35] In addition, the etching cycle can also affect the emission intensity; Figure S2 indicates the relationship between emission intensity and etching cycles. When the power of the plasma was 100 W, the optimum etching period is 200 cycles.

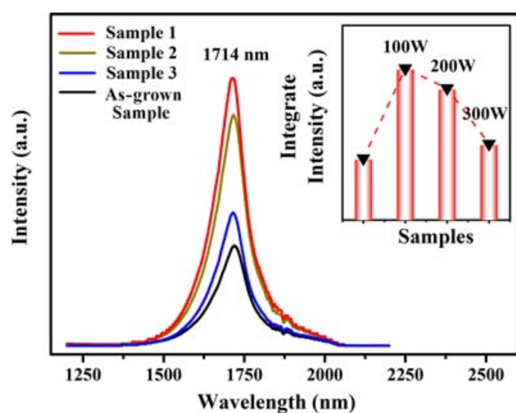

Figure 1. PL spectra of the samples measured at 300 K. The inset shows the integrated intensities of the samples.

The results of the room-temperature PL measurements indicated that N passivation was beneficial for improving the emission efficiency. GaSb has a highly reactive surface and can be easily oxidized at room temperature through the spontaneous reactions of $2GaSb + 3O_2 \rightarrow Ga_2O_3 + Sb_2O_3$ and $2GaSb + Sb_2O_3 \rightarrow Ga_2O_3 + 4Sb$.[36,37] Therefore, the existence of Ga and Sb oxides can be indicators for the surface states. The enhanced emission observed in the experimental data indicated a change in surface states. To support this claim, the chemical compositions of the N plasma-treated samples were investigated by XPS. Figure 2 shows the XPS spectra of the Ga (3d) and Sb (3d) regions for the samples. In the Ga (3d) XPS spectra in Figure 2a, the peaks at 20.7, 20.35, 19.8, 19.2, and 18.9 eV could be indexed to Ga–O bonds in Ga_2O_3 and Ga_2O, Ga–N bonds, Ga–Sb bonds, and Ga–Ga bonds, respectively.[38−41] Ga–O and Ga–Sb bonds were observed in the XPS spectrum of the as-grown GaSb sample because of the native oxide layer covering the GaSb surface.[38,39,42] After N passivation, XPS peaks characteristic of Ga–O bonds in Ga_xO_y were not observed, which indicated the complete removal of the surface oxide. The disappearance of XPS peaks of Ga–O bonds correlated with the emergence of peaks of Ga–N bonds at 19.8 eV in the XPS spectra of all N passivated samples. This indicated that N plasma treatment broke the Ga–O bonds in Ga_2O_3 and Ga_2O and replaced them with Ga–N bonds.[39,40] At a higher plasma power of 200 W (sample 2), in addition to Ga–N bonds, a peak was observed at 18.9 eV, which could be assigned to Ga–Ga bonds, whereas the intensity of the Ga–Sb bond decreased. Increasing the plasma power to 300 W (sample 3) caused the intensity of the peak of Ga–Ga bonds to increase. The presence of Ga–Ga bonds suggested that Ga clusters were formed at the surface of GaSb.[16,41,42] Figure 2b shows the Sb (3d) XPS spectra of the samples. In the spectrum of the as-grown GaSb sample, peaks characteristic of Sb–O, Sb–Sb, and Sb–Ga bonds were observed at 540.1, 537.8, and 537.1 eV, respectively.[16,28,38,39,43] These peaks arose from the presence of the surface oxide, Sb clusters existing between the interface of the surface oxide and GaSb substrate, and the GaSb substrate, respectively.[19,36,37] After N passivation (100 W), peaks of Sb–O bonds and Sb–Sb bonds disappeared from the XPS spectra, and peaks of Sb–N bonds at 539.7 eV were observed.[44] However, increasing the plasma power to 200 or 300 W again resulted in the emergence of peaks of Sb–Sb bonds which were related to Sb clusters. These results indicated the decomposition of the oxide layer and the formation of N-related bonds. The observation of Ga and Sb clusters indicated that excess plasma power harmed the GaSb surface and caused surface defects. Thus, the XPS results suggested that N passivation could suppress surface states and that an appropriate plasma power during the PEALD process was essential.

To explain the increase in NBE and the underlying physical mechanism, low-temperature and temperature-dependent PL measurements were carried out. Figure 3a shows the PL emission of the samples at 20 K. Six PL emission peaks were detected in all samples. According to the characteristic energies of excitonic emission,[45−47] the exciton emission peaks at 0.802 and 0.81 eV can be assigned to free exciton A (FX-a) and free exciton B (FX-b), respectively. The other emission peaks can be assigned to bound exciton emission (BE, 0.795 eV), the native acceptor (A, 0.778 eV) level from the conduction band to the acceptor (BA), or donor–acceptor pair transitions, the acceptor transition (B, 0.758 eV) related to the complex $V_{Ga}Ga_{Sb}V_{Ga}$,[47] and the first-order phonon replica of the native acceptor (A-LO, 0.749 eV).[47,48] The FX-related emission of sample 1 was the highest of all samples. Figure 3b,c shows atomic force microscope (AFM) images of the as-grown GaSb sample and sample 1, respectively. The white raised particles on surface of the GaSb sample were considered to be the native oxide on the GaSb substrate. The surface roughness measure-

DOI: 10.1021/acsomega.7b01783
ACS Omega 2018, 3, 4412−4417

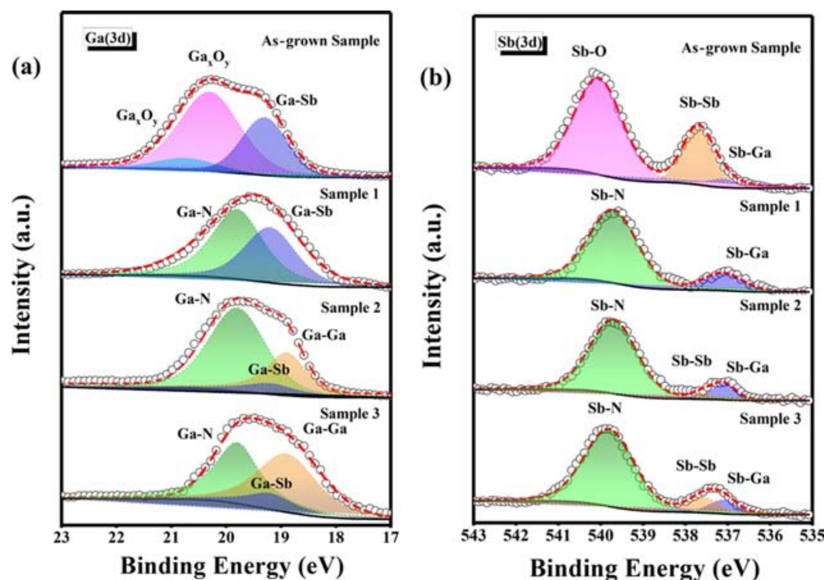

Figure 2. XPS spectra of the (a) Ga (3d) and (b) Sb (3d) regions for the samples.

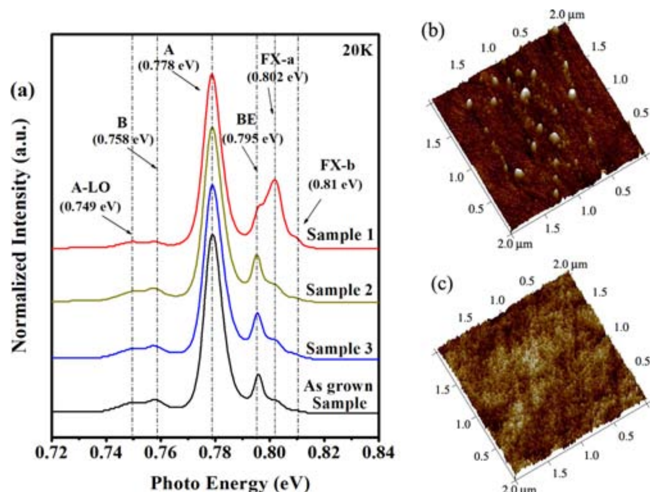

Figure 3. (a) Low-temperature PL spectra of the samples (20 K), and AFM images of the (b) as-grown GaSb sample and (c) sample 1.

ment (RMS) of the GaSb sample was 0.811 nm. N passivation removed the native oxide, so the surface of sample 1 was smoother (RMS of 0.502 nm). The samples exhibited different surface morphologies in the AFM images in Figure S3, thus the surface of GaSb was sensitive to the power of the N plasma.

The as-grown GaSb sample and sample 1 exhibited differing results in both low-temperature PL measurements and AFM observations. Thus, these two samples were further investigated to better understand the origin of the FX emission and the relationship among FX, BE, and A. Temperature-dependent PL measurements were carried out on the as-grown GaSb sample and sample 1 from 20 to 200 K, as shown in Figures 4 and 5, respectively. For the GaSb sample, increasing the temperature led to gradual red shifts and decreases in the intensities of the emissions of FX, BE, and A. The low-temperature (20 K) PL spectrum could be well-fitted by five individual Gaussian peaks, as shown in Figure 4b. The emission of peak A was dominant, but its intensity decreased faster than those of the other emissions. When the temperature increased to 160 K, the emission of A became totally quenched, as shown in Figure 4a.

Figure 4c shows the peak positions of FX, BE, and A, as a function of temperature. The photon energies of these emissions could be well-fitted by the Varshni empirical equation: $E(T) = E_0 - \alpha T^2/(T + \beta)$.[49] As the temperature increased, the bound excitons had sufficient thermal energy to dissociate and become free excitons, similar to the phenomena in other semiconductors.[50] Thus, the emission of the as-grown GaSb sample was dominated by FX at 200 K. Figure 5 shows the temperature-dependent PL spectra of sample 1. Compared with the as-grown GaSb sample, as well as the enhanced FX-a emission, FX-b emission was also observed, as shown in Figure 5b. The intensities of the FX, BE, and A emissions decreased continuously with the increasing temperature. However, the emission of A was quenched at 180 K, as shown in Figure 5a. The trends in the temperature-dependent emission peaks were the same as those for the as-grown GaSb sample. At higher temperature, the emission of sample 1 was also dominated by FX, as shown in Figure 5c.

Figure 6 shows energy band diagrams which better illustrate the physical mechanism of the improved NBE after N passivation. In this experiment, the undoped GaSb substrate was a p-type semiconductor because of its intrinsic defects, and its Fermi energy level was located at higher energy than that of the valence band. The surface states can create a space charge region and strong surface band downward bending because of Fermi energy level pinning. Consequently, photogenerated electron−hole pairs will be separated. Subsequently, the number of excitons and thus the intensity of exciton-related emission will reduce, as shown in Figure 6a. Figure 6b shows that surface states are suppressed by N passivation, thereby shortening the space charge region. The number of excitons and thus the intensity of exciton-related emission would increase, such as FX. This is consistent with previous reports.[50,51] However, the passivation greatly depends on the plasma power. Surface treatment at excess plasma power leads to surface defects such as Ga and Sb clusters and induces many nonradiative recombination centers. Thus, varying the plasma power can tune the surface states and influence the emission efficiency.

DOI: 10.1021/acsomega.7b01783
ACS Omega 2018, 3, 4412−4417

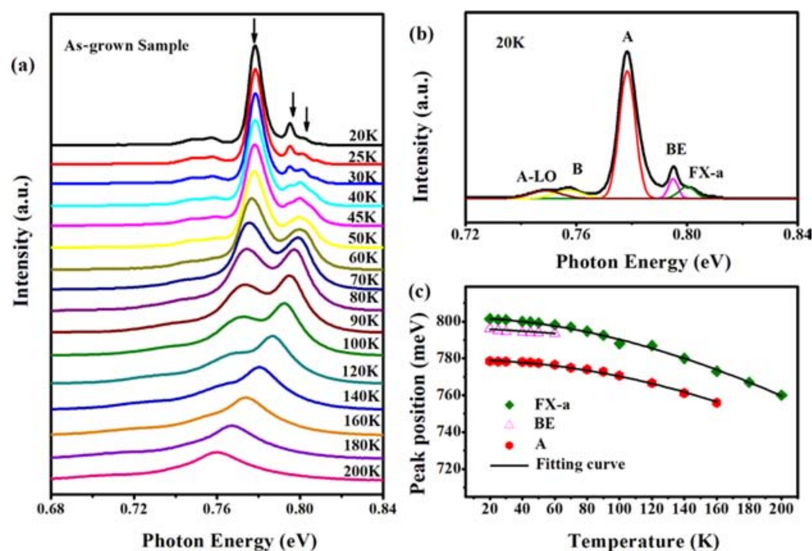

Figure 4. (a) Temperature-dependent PL spectra of the as-grown GaSb sample, (b) 20 K PL spectrum of the as-grown GaSb sample, and (c) temperature-dependent peak positions of the three emission bands of the as-grown GaSb sample.

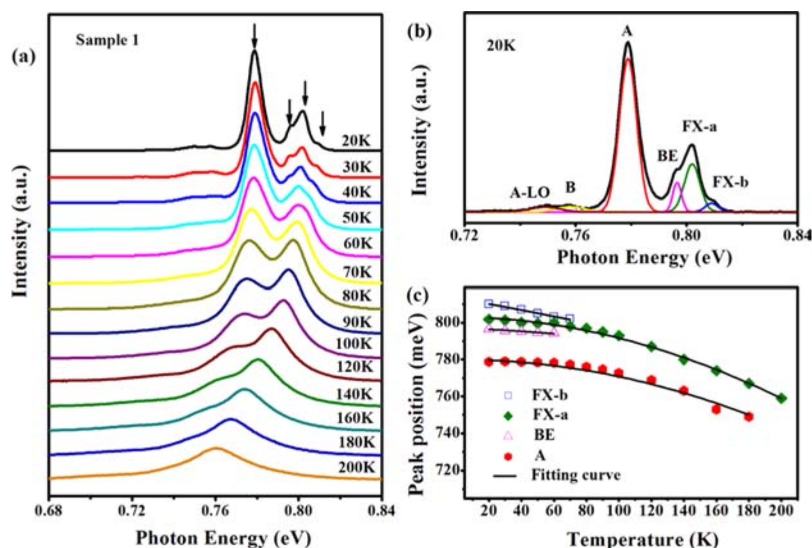

Figure 5. (a) Temperature-dependent PL spectra of sample 1, (b) 20 K PL spectrum of sample 1, and (c) temperature-dependent peak positions of the four emission bands of sample 1.

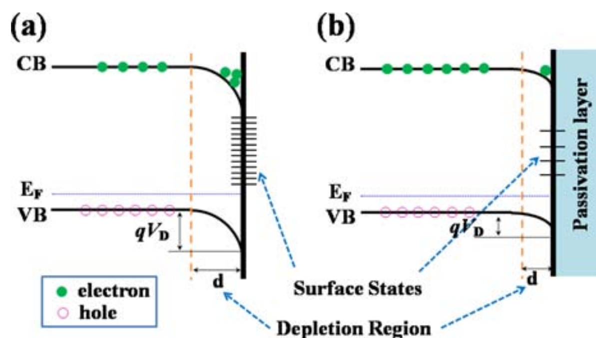

Figure 6. Energy band diagrams of the GaSb sample (a) with and (b) without N passivation.

3. CONCLUSIONS

GaSb substrates were treated by N plasma in a PEALD process, in which the plasma power was varied between 100 and 300 W. The morphology and optical properties of the samples were investigated. It was confirmed that surface states related to the surface oxide layer were removed by N plasma treatment. An optimal plasma power of 100 W was beneficial for reducing the density of surface states, which could alter the surface chemical bonding and enhance the emission from GaSb. Excess plasma power caused the formation of Ga or Sb clusters, which reintroduced and/or increased the amount of surface defects. N plasma treatment induced FX emission. Low-temperature and temperature-dependent PL measurements demonstrated that the FX emission was the cause of the enhanced PL. N plasma treatment is therefore an effective method for restraining surface states, to improve the performance of GaSb-based materials and devices.

4. EXPERIMENTAL SECTION

A GaSb substrate was used for the passivation experiment; the lattice orientation of GaSb was (400). The N passivation of

DOI: 10.1021/acsomega.7b01783
ACS Omega 2018, 3, 4412−4417

GaSb samples was performed during PEALD (LabNano PE plasma/thermal ALD—Ensure Nanotech, Beijing, P. R. China). During the passivation process, high-purity ammonia (NH_3) was used as the nitrogen source, and the number of etching cycles was fixed at 100, 200, 300, or 400. The power of the plasma generator was set at 100, 200, or 300 W. Prior to N passivation, the GaSb samples were washed with deionized water to remove impurities from their surfaces. Samples 1, 2, and 3 were obtained using plasma powers of 100, 200, and 300 W, respectively. For comparison, an undoped GaSb substrate was also prepared for use as a reference sample.

The morphologies of the samples were characterized using a Multimode 8 AFM. For PL measurements, the PL emission was dispersed by a HORIBA iHR550 spectrometer and subsequently detected by an InGaAs detector. During PL measurements, a semiconductor diode laser with a wavelength of 655 nm was used as the excitation source. A standard phase lock-in amplifier technique was used to enhance the signal-to-noise ratio. The excitation power was fixed at 80 mW, and the spot area of the laser was approximately 0.4 cm^2 during the temperature-dependent PL measurements. To evaluate the changes in the GaSb surface composition after N plasma exposure, XPS measurements were obtained using a Thermo Scientific K-Alpha instrument, with Al Kα radiation ($h\nu$ = 1468.60 eV) as the X-ray source. All XPS spectra were calibrated using the C 1s peak at 284.8 eV.

■ ASSOCIATED CONTENT

Supporting Information

The Supporting Information is available free of charge on the ACS Publications website at DOI: 10.1021/acsomega.7b01783.

> Normalized room-temperature PL spectra, etching cycles dependent room-temperature PL spectra, and AFM images of the as-grown GaSb sample and samples 1−3 (PDF)

■ AUTHOR INFORMATION

Corresponding Authors

*E-mail: zpweicust@126.com (Z.P.).
*E-mail: chen.r@sustc.edu.cn (R.C.).

ORCID

Xuan Fang: 0000-0003-2290-4951
Yongfeng Li: 0000-0002-9725-0692
Bin Yao: 0000-0003-0748-3220
Rui Chen: 0000-0002-0445-7847

Notes

The authors declare no competing financial interest.

■ ACKNOWLEDGMENTS

This work was supported by the National Natural Science Foundation of China (61404009, 61474010, 61574022, 61504012, 61674021, 11404219, 11404161, 11574130, and 11674038), the Foundation of State Key Laboratory of High Power Semiconductor Lasers, the Developing Project of Science and Technology of Jilin Province (20160519007JH, 20160520117JH, 20160101255JC, 20160204074GX, and 20170520117JH), and the National 1000 plan for Young Talents and Shenzhen Science and Technology Innovation Committee (projects nos. JCYJ20150630162649956, JCYJ20150930160634263, and KQTD2015071710313656).

■ REFERENCES

(1) Dan, Y.; Seo, K.; Takei, K.; Meza, J. H.; Javey, A.; Crozier, K. B. Dramatic Reduction of Surface Recombination by in situ Surface Passivation of Silicon Nanowires. *Nano Lett.* **2011**, *11*, 2527−2532.

(2) Gamalski, A. D.; Tersoff, J.; Kodambaka, S.; Zakharov, D. N.; Ross, F. M.; Stach, E. A. The Role of Surface Passivation in Controlling Ge Nanowire Faceting. *Nano Lett.* **2015**, *15*, 8211−8216.

(3) Tan, H.; Jain, A.; Voznyy, O.; Lan, X.; de Arquer, F. P. G.; Fan, J. Z.; Quintero-Bermudez, R.; Yuan, M.; Zhang, B.; Zhao, Y.; Fan, F.; Li, P.; Quan, L. N.; Zhao, Y.; Lu, Z.-H.; Yang, Z.; Hoogland, S.; Sargent, E. H. Efficient and Stable Solution-Processed Planar Perovskite Solar Cells via Contact Passivation. *Science* **2017**, *355*, 722−726.

(4) Zhu, S.; Shao, J.; Song, Y.; Zhao, X.; Du, J.; Wang, L.; Wang, H.; Zhang, K.; Zhang, J.; Yang, B. Investigating the Surface State of Graphene Quantum Dots. *Nanoscale* **2015**, *7*, 7927−7933.

(5) Klaumünzer, M.; Hübner, J.; Spitzer, D.; Kryschi, C. Surface Functionalization and Electrical Discharge Sensitivity of Passivated Al Nanoparticles. *ACS Omega* **2017**, *2*, 52−61.

(6) Ludeke, R. Sb-Induced Surface States on (100) Surfaces of III-V Semiconductors. *Phys. Rev. Lett.* **1977**, *39*, 1042−1045.

(7) Nishida, M. Energy Distribution of Dangling-Orbital Surface States on the (110) Surface of III-V Compounds. *Phys. Status Solidi B* **1980**, *99*, K39.

(8) Fang, X.; Wei, Z.; Yang, Y.; Chen, R.; Li, Y.; Tang, J.; Fang, D.; Jia, H.; Wang, D.; Fan, J.; Ma, X.; Yao, B.; Wang, X. Ultraviolet Electroluminescence from ZnS@ZnO Core−Shell Nanowires/p-GaN Introduced by Exciton Localization. *ACS Appl. Mater. Interfaces* **2016**, *8*, 1661−1666.

(9) Li, G.; Chen, T.; Yan, B.; Ma, Y.; Zhang, Z.; Yu, T.; Shen, Z.; Chen, H.; Wu, T. Tunable Wettability in Surface-Modified ZnO-based Hierarchical Nanostructures. *Appl. Phys. Lett.* **2008**, *92*, 173104.

(10) Li, M.; Xing, G.; Ah Qune, L. F. N.; Xing, G.; Wu, T.; Huan, C. H. A.; Zhang, X.; Sum, T. C. Tailoring the Charge Carrier Dynamics in ZnO Nanowires: The Role of Surface hole/electron Traps. *Phys. Chem. Chem. Phys.* **2012**, *14*, 3075−3082.

(11) Wu, K.; Bera, A.; Ma, C.; Du, Y.; Yang, Y.; Li, L.; Wu, T. Temperature-Dependent Excitonic Photoluminescence of Hybrid Organometal Halide Perovskite Films. *Phys. Chem. Chem. Phys.* **2014**, *16*, 22476−22481.

(12) Preisler, E. J.; Strittmatter, R. P.; McGill, T. C.; Hill, C. J. Nitridation of Epitaxially Grown 6.1 Å Semiconductors Studied by X-ray Photoelectron Spectroscopy. *Appl. Surf. Sci.* **2004**, *222*, 6−12.

(13) Hui, Z.; Qin, X.; Cheng, L.; Azcatl, A.; Kim, J.; Wallace, R. M. Remote Plasma Oxidation and Atomic Layer Etching of MoS_2. *ACS Appl. Mater. Interfaces* **2016**, *8*, 19119−19126.

(14) Drygaś, M.; Jeleń, P.; Bućko, M. M.; Olejniczak, Z.; Janik, J. F. Ammonolytical Conversion of Microcrystalline Gallium Antimonide GaSb to Nanocrystalline Gallium Nitride GaN: Thermodynamics vs. Topochemistry. *RSC Adv.* **2015**, *5*, 82576−82586.

(15) Kunitsyna, E. V.; L'vova, T. V.; Dunaevskii, M. S.; Terent'ev, Y. V.; Semenov, A. N.; Solov'ev, V. A.; Meltser, B. Y.; Ivanov, S. V.; Yakovlev, Y. P. Wet Sulfur Passivation of GaSb(100) Surface for Optoelectronic Applications. *Appl. Surf. Sci.* **2010**, *256*, 5644−5649.

(16) Chu, R. L.; Chiang, T. H.; Hsueh, W. J.; Chen, K. H.; Lin, K. Y.; Brown, G. J.; Chyi, J. I.; Kwo, J.; Hong, M. Passivation of GaSb Using Molecular Beam Epitaxy Y_2O_3 to Achieve Low Interfacial Trap Density and High-Performance Self-Aligned Inversion-Channel p-Metal-Oxide-Semiconductor Field-Effect-Transistors. *Appl. Phys. Lett.* **2014**, *105*, 182106.

(17) Bose, R.; Bera, A.; Parida, M. R.; Adhikari, A.; Shaheen, B. S.; Alarousu, E.; Sun, J. Y.; Wu, T.; Bakr, O. M.; Mohammed, O. F. Real-Space Mapping of Surface Trap States in CIGSe Nanocrystals Using 4D Electron Microscopy. *Nano Lett.* **2016**, *16*, 4417−4423.

(18) David, A.; Tian, Y.; Yang, P.; Gao, X.; Lin, W.; Shah, A. B.; Zuo, J.-M.; Prellier, W.; Wu, T. Colossal Positive Magnetoresistance in Surface-Passivated Oxygen-Deficient Strontium Titanite. *Sci. Rep.* **2015**, *5*, 10255.

(19) Kim, S.; Yoo, S.; Lim, H.; Kim, J.-R.; Jeong, J. K.; Kim, H. J. Fermi-Level Unpinning in Pt/Al_2O_3/GaSb PMOS Capacitors by

DOI: 10.1021/acsomega.7b01783
ACS Omega 2018, 3, 4412−4417

Sulphurization and Rapid Thermal Annealing of GaSb Surfaces. *Appl. Phys. Lett.* **2016**, *109*, 072104.
(20) Chavan, A.; Chandola, A.; Sridaran, S.; Dutta, P. Surface Passivation and Capping of GaSb Photodiode by Chemical Bath Deposition of CdS. *J. Appl. Phys.* **2006**, *100*, 064512.
(21) Zhao, L.; Tan, Z.; Bai, R.; Cui, N.; Wang, J.; Xu, J. Effects of Sulfur Passivation on GaSb Metal−Oxide−Semiconductor Capacitors with Neutralized and Unneutralized $(NH_4)_2S$ Solutions of Varied Concentrations. *Appl. Phys. Express* **2013**, *6*, 056502.
(22) Cleveland, E. R.; Ruppalt, L. B.; Bennett, B. R.; Prokes, S. M. Effect of an in situ Hydrogen Plasma Pre-Treatment on the Reduction of GaSb Native Oxides Prior to Atomic Layer Deposition. *Appl. Surf. Sci.* **2013**, *277*, 167−175.
(23) Zazo, L. J. G.; Montojo, M. T.; Castano, J. L.; Piqueras, J. Chemical Cleaning of GaSb(1,0,0) Surfaces. *J. Electrochem. Soc.* **1989**, *136*, 1480−1484.
(24) Wang, B.; Wei, Z.; Li, M.; Liu, G.; Zou, Y.; Xing, G.; Tan, T. T.; Li, S.; Chu, X.; Fang, F.; Fang, X.; Li, J.; Wang, X.; Ma, X. Tailoring the Photoluminescence Characteristics of p-type GaSb: The Role of Surface Chemical Passivation. *Chem. Phys. Lett.* **2013**, *556*, 182−187.
(25) Parize, R.; Katerski, A.; Gromyko, I.; Rapenne, L.; Roussel, H.; Kärber, E.; Appert, E.; Krunks, M.; Consonni, V. A $ZnO/TiO_2/Sb_2S_3$ Core−Shell Nanowire Heterostructure for Extremely Thin Absorber Solar Cells. *J. Phys. Chem. C* **2017**, *121*, 9672−9680.
(26) Liu, Z. Y.; Kuech, T. F.; Saulys, D. A. A comparative Study of GaSb (100) Surface Passivation by Aqueous and Nonaqueous Solutions. *Appl. Phys. Lett.* **2003**, *83*, 2587.
(27) Murape, D. M.; Eassa, N.; Neethling, J. H.; Betz, R.; Coetsee, E.; Swart, H. C.; Botha, J. R.; Venter, A. Treatment for GaSb Surfaces Using a Sulphur Blended $(NH_4)_2S/(NH_4)_2SO_4$ Solution. *Appl. Surf. Sci.* **2012**, *258*, 6753−6758.
(28) Yang, Z.-X.; Yip, S.; Li, D.; Han, N.; Dong, G.; Liang, X.; Shu, L.; Hung, T. F.; Mo, X.; Ho, J. C. Approaching the Hole Mobility Limit of GaSb Nanowires. *ACS Nano* **2015**, *9*, 9268−9275.
(29) Jin, H. S.; Cho, Y. J.; Seok, T. J.; Kim, D. H.; Kim, D. W.; Lee, S. M.; Park, J.-B.; Yun, D.-Y.; Kim, S. K.; Hwang, C. S.; Park, T. J. Improved Interface Properties of Atomic-Layer-Deposited HfO_2 Film on InP Using Interface Sulfur Passivation with H_2S Pre-Deposition Annealing. *Appl. Surf. Sci.* **2015**, *357*, 2306−2312.
(30) Jin, H. S.; Cho, Y. J.; Lee, S.-M.; Kim, D. H.; Kim, D. W.; Lee, D.; Park, J.-B.; Won, J. Y.; Lee, M.-J.; Cho, S.-H.; Hwang, C. S.; Park, T. J. Interface Sulfur Passivation using H_2S Annealing for Atomic-Layer-Deposited Al_2O_3 Films on an Ultrathin-Body $In_{0.53}Ga_{0.47}As$-on-insulator. *Appl. Surf. Sci.* **2014**, *315*, 178−183.
(31) Seok, T. J.; Cho, Y. J.; Jin, H. S.; Kim, D. H.; Kim, D. W.; Lee, S.-M.; Park, J.-B.; Won, J.-Y.; Kim, S. K.; Hwang, C. S.; Park, T. J. High Quality Interfacial Sulfur Passivation via H_2S Pre-Deposition Annealing for an Atomic-Layer Deposited HfO_2 Film on a Ge Substrate. *J. Mater. Chem. C* **2016**, *4*, 850−856.
(32) Guo, Y.; Lin, L.; Robertson, J. Nitrogen Passivation at $GaAs:Al_2O_3$ Interfaces. *Appl. Phys. Lett.* **2013**, *102*, 091606.
(33) Alekseev, P. A.; Dunaevskiy, M. S.; Ulin, V. P.; Lvova, T. V.; Filatov, D. O.; Nezhdanov, A. V.; Mashin, A. I.; Berkovits, V. L. Nitride Surface Passivation of GaAs Nanowires: Impact on Surface State Density. *Nano Lett.* **2015**, *15*, 63−68.
(34) Ge, X.; Wang, D.; Gao, X.; Fang, X.; Niu, S.; Gao, H.; Tang, J.; Wang, X.; Wei, Z.; Chen, R. Localized States Emission in Type-I GaAsSb/AlGaAs Multiple Quantum Wells Grown by Molecular Beam Epitaxy. *Phys. Status Solidi RRL* **2007**, *11*, 1700001.
(35) Fang, X.; Wei, Z.; Chen, R.; Tang, J.; Zhao, H.; Zhang, L.; Zhao, D.; Fang, D.; Li, J.; Fang, F.; Chu, X.; Wang, X. Influence of Exciton Localization on the Emission and Ultraviolet Photoresponse of ZnO/ZnS Core−Shell Nanowires. *ACS Appl. Mater. Interfaces* **2015**, *8*, 10331−10336.
(36) Dutta, P. S.; Bhat, H. L.; Kumar, V. The Physics and Technology of Gallium Antimonide: An Emerging Optoelectronic Material. *J. Appl. Phys.* **1997**, *81*, 5821.
(37) Ali, A.; Madan, H. S.; Kirk, A. P.; Zhao, D. A.; Mourey, D. A.; Hudait, M. K.; Wallace, R. M.; Jackson, T. N.; Bennett, B. R.; Boos, J. B.; Datta, S. Fermi Level Unpinning of GaSb (100) Using Plasma Enhanced Atomic Layer Deposition of Al_2O_3. *Appl. Phys. Lett.* **2010**, *97*, 143502.
(38) Lebedev, M. V.; Kunitsyna, E. V.; Calvet, W.; Mayer, T.; Jaegermann, W. Sulfur Passivation of GaSb(100) Surfaces: Comparison of Aqueous and Alcoholic Sulfide Solutions Using Synchrotron Radiation Photoemission Spectroscopy. *J. Phys. Chem. C* **2013**, *117*, 15996−16004.
(39) Cotirlan, C.; Ghita, R. V.; Negrila, C. C.; Logofatu, C.; Frumosu, F.; Lungu, G. A. Aspects of Native Oxides Etching on n-GaSb(100) Surface. *Appl. Surf. Sci.* **2016**, *363*, 83−90.
(40) Ould-Metidji, Y.; Bideux, L.; Baca, D.; Gruzza, B.; Matolin, V. Nitridation of GaAs (100) Substrates and Ga/GaAs Systems Studied by XPS Spectroscopy. *Appl. Surf. Sci.* **2003**, *212*, 614−618.
(41) Gao, F.; Lee, S. J.; Chi, D. Z.; Balakumar, S.; Kwong, D.-L. GaAs Metal-Oxide-Semiconductor Device with HfO_2/TaN Gate Stack and Thermal Nitridation Surface Passivation. *Appl. Phys. Lett.* **2007**, *90*, 252904.
(42) Cleveland, E. R.; Ruppalt, L. B.; Bennett, B. R.; Prokes, S. M. Effect of an in situ Hydrogen Plasma Pre-Treatment on the Reduction of GaSb Native Oxides Prior to Atomic Layer Deposition. *Appl. Surf. Sci.* **2013**, *277*, 167−175.
(43) McDonnell, S.; Zhernokletov, D. M.; Kirk, A. P.; Kim, J.; Wallace, R. M. In situ X-ray Photoelectron Spectroscopy Characterization of Al_2O_3/GaSb Interface Evolution. *Appl. Surf. Sci.* **2011**, *257*, 8747−8751.
(44) Haworth, L.; Lu, J.; Hill, P.; Westwood, D. I.; Macdonald, J. E.; Hartmann, N.; Schneider, A.; Zahn, D. R. T. Formation of an Sb−N Compound during Nitridation of InSb (001) Substrates Using Atomic Nitrogen. *J. Vac. Sci. Technol., B: Microelectron. Nanometer Struct.–Process., Meas., Phenom.* **1998**, *16*, 2254.
(45) Bignazzi, A.; Bosacchi, A.; Magnanini, R. Photoluminescence Study of Heavy Doping Effects in Te-doped GaSb. *J. Appl. Phys.* **1997**, *81*, 7540.
(46) Jakowetz, W.; Rühle, W.; Breuninger, K.; Pilkuhn, M. Luminescence and Photoconductivity of Undoped p-GaSb. *Phys. Status Solidi A* **1972**, *12*, 169.
(47) Lee, M.; Nicholas, D. J.; Singer, K. E.; Hamilton, B. A Photoluminescence and Hall-Effect Study of GaSb Grown by Molecular-Beam Epitaxy. *J. Appl. Phys.* **1986**, *59*, 2895.
(48) la Guillaume, C. B. A.; Lavallard, P. Piezoemission of GaSb: Impurities and Bound Excitons. *Phys. Rev. B: Solid State* **1972**, *5*, 4900−4910.
(49) Varshni, Y. P. Temperature Dependence of the Energy Gap in Semiconductors. *Physica* **1967**, *34*, 149−154.
(50) Liu, K. W.; Chen, R.; Xing, G. Z.; Wu, T.; Sun, H. D. Photoluminescence characteristics of high quality ZnO nanowires and its enhancement by polymer covering. *Appl. Phys. Lett.* **2010**, *96*, 023111.
(51) Li, D.; Zhang, J.; Xiong, Q. Surface Depletion Induced Quantum Confinement in CdS Nanobelts. *ACS Nano* **2012**, *6*, 5283−5290.

DOI: 10.1021/acsomega.7b01783
ACS Omega 2018, 3, 4412−4417